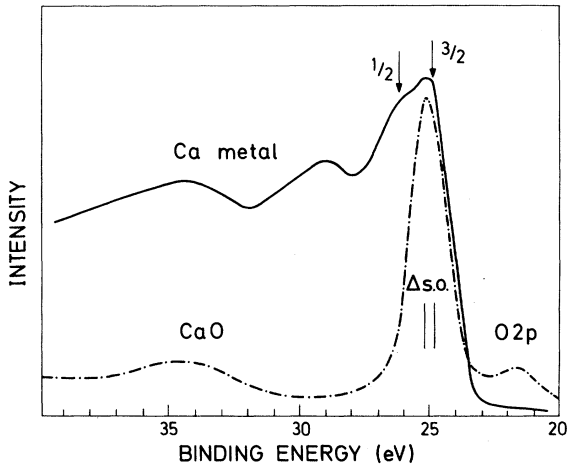

FIG. 4. The Ca 3*p* spectrum in Ca metal and in CaO. The spectra have been aligned.

(ii) As a consequence of the unusually high coupling strength of the core holes to the excitation spectrum of these metals we would expect very high *extra-atomic* relaxation energies. The extra-atomic relaxation energies of Ca, Sr, and Ba are indeed only surpassed by those of Li according to a recent study by Johansson and Mårtensson[15] if one disregards the transition metals.

(iii) A reduction in the coupling strength should result in a reduction of the apparent spin-orbit splitting. This is indeed observed if we compare the 3*p* spectrum of Ca with that of CaO in Fig. 4. The single line in CaO is expected for an unresolved spin-orbit splitting of 0.35 eV.

[a]Permanent address: University of Uppsala, Uppsala, Sweden.

[b]Permanent address: The Hebrew University, Jerusalem, Israel.

[1]See, e.g., D. A. Shirley, in *Topics in Applied Physics*, edited by M. Cardona and L. Ley (Springer, Berlin, 1978), Vol. 26, p. 165.

[2]J. W. Gadzuk, in *Photoemission and the Electronic Properties of Surfaces*, edited by B. Feuerbacher, B. Fitton, and R. F. Willis (Wiley, Chichester, N. Y., 1978), p. 111.

[3]B. I. Lundquist, Phys. Kondens. Mater. 6, 167 (1967).

[4]D. C. Langreth, in *Collective Properties of Physical Systems*, edited by B. Lundquist and S. Lundquist (Academic, New York, 1974), p. 210.

[5]W. J. Pardee, G. D. Mahan, D. E. Eastman, R. A. Pollak, L. Ley, F. R. McFeely, S. P. Kowalczyk, and D. A. Shirley, Phys. Rev. B 11, 3614 (1975).

[6]D. R. Penn, Phys. Rev. Lett. 38, 1429 (1977).

[7]P. Steiner, H. Höchst, and S. Hüfner, Z. Phys. B 30, 129 (1978).

[8]J. Langkowski, J. Phys. D 8, 2058 (1975).

[9]H. Raether, in *Springer Tracts in Modern Physics*, edited by G. Höhler (Springer, Berlin, 1965), Vol. 38, p. 84.

[10]P. A. Wolff, Phys. Rev. 95, 56 (1954).

[11]C. Powell, Surf. Sci. 44, 29 (1974).

[12]W. Schmitz, B. Brenckmann, and W. Mehlhorn, J. Phys. B 9, L493 (1976); W. Mehlhorn, B. Brenckmann, and D. Hausmann, Phys. Scr. 16, 177 (1977).

[13]L. Ley, S. P. Kowalczyk, F. R. McFeely, and D. A. Shirley, Phys. Rev. B 10, 4881 (1974).

[14]N. Shevchik, J. Tejeda, M. Cardona, and D. W. Langer, Phys. Status Solidi (b) 59, 87 (1973).

[15]B. Johansson and N. Mårtensson, private communication.

Surface-Enchanced Raman Scattering from Pyridine on Ag(111)

P. N. Sanda, J. M. Warlaumont, J. E. Demuth, J. C. Tsang, K. Christmann,[a] and J. A. Bradley

IBM T. J. Watson Research Center, Yorktown Heights, New York 10598

(Received 21 July 1980)

This Letter reports the first ultrahigh-vacuum study of surface-enhanced Raman scattering from pyridine adsorbed on a clean single-crystal silver surface containing a smooth modulation (1 μm periodicity) to allow optical coupling to surface plasmon polaritons. A large mode-selective enhancement ($\sim 10^4$) of the Raman signal from the first monolayer is observed at surface-plasmon-polariton resonance. Coverages greater than one monolayer show a smaller enhancement ($\sim 10^2$).

PACS numbers: 78.30.Jw

Surface-enhanced Raman scattering has been observed in electrochemical cell systems,[1] tunnel-junction structures,[2,3] discontinuous films,[4] small particles in solution,[5] and recently for surfaces prepared in ultrahigh vacuum (UHV).[6-8] Recent UHV experiments have used the photoreac-

tion of iodine on Ag to form silver balls,[6] films evaporated at low temperatures,[7] or sputter-damaged polycrystalline samples.[8] However, all experiments reported including those performed in UHV have required deliberate roughening of the surface in order to obtain a measurable signal from a monolayer of an adsorbate, thereby complicating the interpretation of these results.

Here we present surface Raman scattering results using a clean, essentially (111)-oriented Ag surface with a controlled surface modulation (wavelength = 10 000 Å). This surface contains a small-amplitude, approximately sinusoidal modulation (height ~ 1000 Å), which provides a well-defined surface periodicity to allow optical coupling to surface plasmon polaritons, while maintaining minimal deviation from a flat Ag(111) surface. Our experiments are thereby intended to ellucidate the role of surface plasmon polaritons in surface-enhanced Raman scattering. We find a large enhancement ($\sim 10^4$) for the first adsorbed layer, and a comparatively small enhancement ($\sim 10^2$) for further condensed layers. These results demonstrate that such surface-plasmon-polariton–induced Raman scattering is strongly localized to the first molecular layer.

The experiments were performed in an ion– and Ti-sublimator–pumped vacuum system (typical base pressure of 2×10^{-10} Torr) having facilities for low-energy electron diffraction (LEED), Auger-electron spectroscopy (AES), and Ar^+ sputtering. Reagent-grade pyridine was used. The Raman spectra shown here were measured at 80 K with the 5145-Å line from an Ar^+ laser, although measurements were also made with the 4880-Å Ar^+ line and the 5309-Å line from a Kr^+ laser. Standard backscattering geometry was used, with light collected over a solid angle of 45°. The scattered light was analyzed by a conventional double-grating monochromator operating at 6 cm^{-1} resolution. Given our operating conditions, the threshold enhancement for detecting a monolayer was $\sim 5\times10^2$.

Although AES was used to monitor and characterize surface cleanliness, uv photoemission spectroscopy (UPS) was utilized to calibrate relative adsorbate coverages and to allow a clear delineation between chemisorbed and physisorbed pyridine. These measurements were performed in a separate vacuum system, on the same Ag crystal, with use of a differentially pumped He-resonance lamp ($h\nu = 21.2$ eV) and a double-pass cylindrical-mirror analyzer.[9]

The Ag crystal was spark cut, mechanically polished, chemically polished [chromic acid and HCl (Ref. 10)], then several UHV sputtering/annealing cycles were used to remove C and S impurities from the bulk and to segregate dislocation defects to the surface. A final chemical polish left the crystal with a mirrorlike finish, free of etch pits. The 10 000-Å periodic surface modulation was then fabricated into a 4×4 mm^2 area of the 8×6 mm^2 face of the crystal, with the modulation wave vector $\vec{K}_s$ oriented along the (110) direction. This structure was fabricated by first creating a photoresist pattern on the sample with use of x-ray lithography techniques followed by chemical polishing to remove about 3000 Å of material in the unmasked regions (50%). The photoresist was then dissolved and the sample was repeatedly argon sputter etched and annealed in UHV ($T \sim 500$ K). This preparation also served to reduce the higher-order Fourier components[11] of the profile, resulting in a sinusoidallike surface (valleys slightly wider than the peaks) with a 10 000 Å wavelength and ~ 1000 Å height as estimated by the LEED beam profiles. The modulated region of the sample showed a well-defined, low-background LEED pattern, comparable to the control region of the sample. Satellite lobes were observed in the beam profiles, which indicated a distribution of steps and terraces parallel to $\vec{K}_s$. The peak in this distribution corresponded to a terrace width to step height ratio of about 10 to 1. The intensity of the main peak relative to the side lobes indicated that roughly 90% of the surface is of (111) orientation. Although such LEED features serve as a guide to the general nature and condition of the surface, they do not provide specific information concerning all types of defects that may exist on an atomic scale.

UPS difference curves, $\Delta N(E)$, in Fig. 1 show the adsorbate-induced changes in emission for consecutive pyridine exposures. The ionization features in Fig. 1 demonstrate a pronounced energy shift starting at coverages above ~ 1.2 L. This increase in binding energy for physisorbed pyridine compared to chemisorbed pyridine is expected. It is attributed to a reduction of the relaxation effects due to molecular polarization, charge transfer, and final-state image-charge screening for the physisorbed layer.[13] This shift can be most reliably seen (light vertical lines) in the lower-lying levels (binding energy ~ 11.5 and 13 eV) which should be least affected by initial-state chemical-bonding effects. The absolute coverage calibration was obtained by taking the total adsorbate-induced intensity of the large peak at

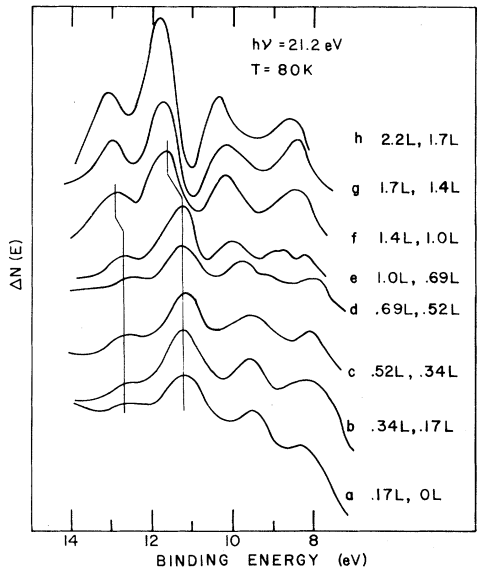

FIG. 1. UPS difference spectra $\Delta N(E)$ for pairs of successive pyridine exposures, as indicated to the right (1 L = 10^{-6} Torr sec), where the ion-gauge pressure reading has been divided by 5.8 to account for the gauge correction (Ref. 12). Spectra e–h have been divided by 2.

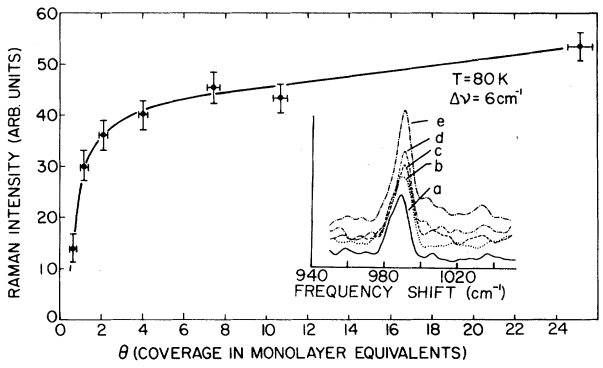

FIG. 2. Raman intensity vs pyridine coverage Θ for the 990-cm^{-1} mode. One monolayer equivalent occurs at 1.2 L exposure as described in the text. Inset: Raman spectra for increasing pyridine exposures: curve a, 1.7 L; curve b, 3.4 L; curve c, 6.9 L; curve d, 19.3 L; curve e, 44 L. The incident laser power is 150 mW.

about 11.5 eV (combination of a_1 and b_2 orbitals)[14] to correspond to one monolayer at 1.2 L exposure.

In order to obtain surface-Raman-scattering signals, it was necessary to couple to surface plasmon polaritons[2] by varying the orientation of the incident radiation with respect to $\vec{K}_s$. For the data presented here, we used p-polarized incident radiation and oriented the sample so that $\vec{K}_s$ was in the plane of incidence. The angle of incidence was set to the minimum in intensity of the direct reflected beam, which corresponds to maximal surface-plasmon-polariton excitation. The Raman-scattered signal for pyridine adsorbed on the modulated portion of the sample was observed as the incident angle was brought to within 5° of this condition. As expected, there was no Raman-scattered signal observed from the flat (control) portion of the sample.

The features found to be observable in the Raman spectrum for chemisorbed pyridine on our modulated Ag(111) surface occurred between 950 and 1050 cm^{-1}. No C-H modes were seen. The carbon-ring deformation modes in the 1300–1600-cm^{-1} range could not be detected. Such features are probably masked by the broad peaks at 1350 cm^{-1} because of trace amounts of amorphous carbon.[15,16] We found these peaks to persist even at carbon levels undetectable by AES. Also, prior to complete annealing, we observed an additional peak at 986 cm^{-1} which we associate with pyridine bound to step sites.

Representative surface Raman spectra for increasing pyridine exposures are shown in the inset in Fig. 2. Compared with the liquid-phase spectra, for which the symmetric (991 cm^{-1}) and the asymmetric (1030 cm^{-1}) ring-breathing modes are of about equal intensity, these spectra show selective enhancement of the symmetric ring-breathing mode for chemisorbed pyridine. It is not until thick condensed layers are obtained (exposure > 20 L) that the asymmetric ring-breathing mode starts to be observed and continues to grow with increasing exposure.

The coverage-dependent Raman intensity $I(\Theta)$ of the 990-cm^{-1} (Fig. 2) peak shows a dramatic increase for the first monolayer relative to higher coverages. The incremental enhancement given by $dI/d\Theta$ is plotted against Θ in Fig. 3; the solid points were obtained experimentally, while the open points correspond to theory as discussed below. The enhancement for the first layer is $\sim 10^4$ from comparative Raman measurements with liquid pyridine, under the same optics and operating conditions and if one assumes the liquid-phase packing density for chemisorbed pyridine. $dI/d\Theta$ drops off quite rapidly in the region from Θ = 1–2 monolayers, and for larger values of Θ levels off to an asymptotic value of ~3% of the monolayer value.

A theoretical model by Kirtley, Jha, and Tsang[17] predicts two mechanisms contributing to the sur-

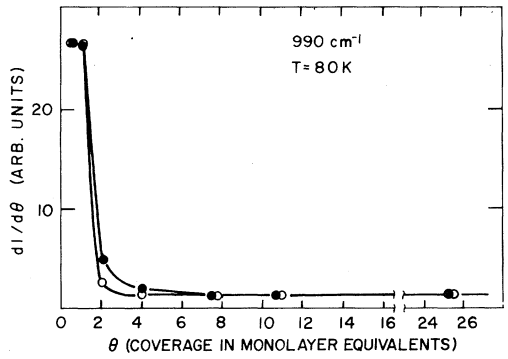

FIG. 3. Incremental enhancement factor $dI/d\Theta$, as a function of coverage as determined from Fig. 2 (solid circles) and predicted by theory (open circles, Ref. 17). For modeling the theoretical distance dependence we used a pyridine interlayer spacing of 5 Å (Ref. 19) and a Ag-pyridine barrier height of 0.25 V (Ref. 17).

face-enhanced Raman-scattering process for a molecule adsorbed on a sinusoidal grating: (1) There is a long-range contribution, extending several thousand angstroms away from the surface, which is due to enhancement of the direct scattering intensity by the large electric field at surface-plasmon-polariton resonance.[18] This classical field enhancement is predicted by the theory to provide an enhancement of the Raman signal by a factor of 10^2 to 10^4. (2) The second term is associated with a short-range mechanism, which is very localized to the surface region. This effect arises from the large oscillating charge density in the molecular layer at surface-plasmon-polariton resonance, which is modulated by the molecular vibrations to produce a modulated surface dipole moment. This term represents a Raman-scattering process with a surface-plasmon-polariton intermediate state. At atomic distances, the theory predicts the total combined Raman enhancement factor to be between 10^4 and 10^6.

We have compared our results to the distance-dependent theory, assuming the uniform bulk packing density for pyridine. In Fig. 3 we have scaled the short-range and long-range parts of the theoretical contribution (open circles) to the experimental values (closed circles) at $\Theta = 1$ and $\Theta = 20$, respectively. Our coverage-dependent results qualitatively agree with this theory. However, because of our limits of sensitivity, we cannot exclude additional short-range enhancements ($\lesssim 10^2$) associated with mechanisms not involving surface plasmons. One proposed origin for the short-range enhancement is associated with bonding to isolated Ag atoms.[7] We do not expect an appreciable density of such adatom sites after annealing our surface. Our results also differ from the weak distance dependence observed by Rowe *et al.*[6] This difference may arise from the possibility that the electric field at their 1000-Å balls is stronger than the field at our weakly modulated surface, which would suggest a larger classical field enhancement for their system.

In conclusion, by studying pyridine adsorption on an essentially (111)-oriented Ag surface with a well-defined surface topography, we have obtained experimental results showing that surface-plasmon-polariton excitations can contribute to a large surface-enhanced Raman-scattering signal for certain adsorbate modes. The enhancement which we observe is strongly distance dependent, being 10^4 for the chemisorbed pyridine and a factor of ~100 weaker for subsequent pyridine layers.

We would like to thank J. R. Kirtley and Professor S. S. Jha for many helpful discussions. We also acknowledge M. T. Prikas and A. Marx for their technical assistance. One of us (P.N.S.) thanks Professor R. P. Merrill, Professor J. W. Wilkins, and D. E. Eastman for their advice and encouragement. This work has been supported in part by the U. S. Office of Naval Research.

---

[a]Permanent address: Institut für Physikalische Chemie der Universität München, München, West Germany.

[1]M. Fleischmann, P. J. Hendra, and A. J. McQuillan, Chem. Phys. Lett. 26, 163 (1974); D. L. Jeanmaire and R. P. Van Duyne, J. Electroanal. Chem. 84, 1 (1977).

[2]J. C. Tsang, J. R. Kirtley, and J. A. Bradley, Phys. Rev. Lett. 43, 772 (1979).

[3]J. C. Tsang and J. R. Kirtley, Solid State Commun. 30, 617 (1979).

[4]C. Y. Chen, E. Burstein, and S. Lundquist, Solid State Commun. 32, 63 (1979); H. Seki and M. R. Philpott, to be published.

[5]J. A. Creighton, C. G. Blatchford, and M. G. Albrecht, J. Chem. Soc. Faraday Trans. II 75, 790 (1979).

[6]J. E. Rowe, C. V. Shank, D. A. Zwemer, and C. A. Murray, Phys. Rev. Lett. 44, 1770 (1980).

[7]T. A. Wood and M. V. Klein, J. Vac. Sci. Technol. 16, 459 (1979); I. Pockrand and A. Otto, to be published.

[8]R. R. Smardzewski, R. J. Colton, and J. S. Murday, Chem. Phys. Lett. 68, 53 (1979).

[9]J. E. Demuth, Surf. Sci. 69, 365 (1977).

[10]H. J. Levinstein and W. H. Robinson, J. Appl. Phys. 33, 3149 (1962).

[11]P. S. Maiya and J. M. Blakely, Appl. Phys. Lett. 7,

60 (1965).
[12]This corresponds to the ionization-gauge correction for benzene as obtained from the gas sensitivity tables supplied with our Varian ion gauge.
[13]J. E. Demuth and D. E. Eastman, Phys. Rev. Lett. 32, 1123 (1974).
[14]W. von Niesen, G. H. F. Diercksen, and L. S. Cederbaum, Chem. Phys. 10, 345 (1975).
[15]M. R. Mahony, M. W. Howard, and R. P. Cooney, Chem. Phys. Lett. 71, 59 (1980).
[16]J. C. Tsang, J. E. Demuth, P. N. Sanda, and J. R. Kirtley, to be published.
[17]J. R. Kirtley, S. S. Jha, and J. C. Tsang, to be published; S. S. Jha, J. R. Kirtley, and J. C. Tsang, Phys. Rev. B 22, 3973 (1980).
[18]A. Girlando, M. R. Philpott, D. Heitmann, J. D. Swalen, and R. Santo, J. Chem. Phys. 72, 5187 (1980).
[19]C. S. G. Biswas, Indian J. Phys. 32, 13 (1958).

Phase-Slip Shot Noise at the Two-Dimensional Superconducting Transition: Evidence for Vortices?

R. F. Voss, C. M. Knoedler, and P. M. Horn
IBM Thomas J. Watson Research Center, Yorktown Heights, New York 10598
(Received 11 August 1980)

This Letter reports the results of a systematic study of the current-induced noise at the superconducting transition in thin, high-resistivity films of aluminum and tin. Analysis of the noise suggests that the onset of resistance is due to discrete phase slips of magnitude less than 2π. The results are discussed in terms of the vortex unbinding models of the superconducting transition in two dimensions.

PACS numbers: 74.40.+k, 72.70.+m, 73.60.Ka

In this Letter we describe the results of a systematic study of the voltage noise in dirty superconducting films in the region of the resistive transition.[1] The traditional approach[2] has been to examine the effect of superconducting fluctuations on the normal-state resistance. However, when the fluctuations become sufficiently large, it is more fruitful to examine the mechanism for the onset of resistance from the superconducting state. As we will demonstrate, noise measurements provide a direct measure of the temporal character of the sample resistance and hence represent a unique probe of this mechanism.

The aluminum and tin films used in this study were flash evaporated onto glass substrates in an oxygen atmosphere with use of procedures described by Abeles, Cohen, and Cullen.[3] This technique produces films with small grains (50 Å), high sheet resistances $R_\square \approx 50$–$5000\ \Omega/\square$, and thicknesses less than 100 Å. Typically, a 1000-$\Omega/\square$ Al film would have a zero-temperature London penetration depth $\approx 12\,000$ Å and a coherence length $\xi(0) \approx 120$ Å. Thus, in the vicinity of the resistive transition, a vortex core [area $\approx \xi^2(T)$] contains many grains and much of the granular disorder is washed out. The transition temperature, however, is a strong function of film thickness, grain size, and spacing.[3] Systematic variations across the sample can lead to unusually broad resistive transitions and a resistivity that depends on sample size. We shall discuss only samples that showed no evidence of such macroscopic disorder.

The samples were immersed in liquid helium inside a double Mumetal-shielded Dewar with an ambient magnetic field less than 1.7×10^{-4} Oe. Individually shielded twisted pair leads coupled the sample to a special low-noise field-effect-transistor preamplifier and to external current and voltage connections. The preamplifier output was coupled to a bandpass filter and an ac voltmeter to allow estimation of the voltage-noise spectral density in the frequency range 10–100 kHz. A small dc current I_b (0.5–40 μA) was applied to the sample and the dc voltage V_{dc} and rms noise voltage were digitally recorded and averaged as the temperature was slowly varied.

Representative results for a 380-$\Omega/\square$ Al sample are presented in Fig. 1. The spectral density of the noise at 100 kHz, S_V(100 kHz), and the resistance R are shown versus temperature T for various I_b. The preamplifier background of 1.6×10^{-18} V^2/Hz has been subtracted from S_V. With $I_b = 0$, the increase of S_V with T is given by the usual Johnson- (thermal-) noise result $S_V = 4k_B \times TR(T)$. With $I_b > 0$, a peak appears in S_V in the vicinity of the resistive transition. The width of both the peak in S_V and the resistive transition are strong functions of $R_\square$ with broad peaks and transitions occurring at large values of $R_\square$. As